

Subtle gene modification in mouse ES cells: evidence for incorporation of unmodified oligonucleotides without induction of DNA damage

Marieke Aarts and Hein te Riele*

Division of Molecular Biology, The Netherlands Cancer Institute, Plesmanlaan 121, 1066 CX Amsterdam, The Netherlands

Received February 23, 2010; Revised June 11, 2010; Accepted June 14, 2010

ABSTRACT

Gene targeting by single-stranded oligodeoxyribonucleotides (ssODNs) is a promising tool for site-specific gene modification in mouse embryonic stem cells (ESCs). We have developed an ESC line carrying a mutant *EGFP* reporter gene to monitor gene correction events shortly after exposure to ssODNs. We used this system to compare the appearance and fate of cells corrected by sense or anti-sense ssODNs. The slower appearance of green fluorescent cells with sense ssODNs as compared to anti-sense ssODNs is consistent with physical incorporation of the ssODN into the genome. Thus, the supremacy of anti-sense ssODNs, previously reported by others, may be an artefact of early readout of the *EGFP* reporter. Importantly, gene correction by unmodified ssODNs only mildly affected the viability of targeted cells and did not induce genomic DNA double-stranded breaks (DSBs). In contrast, ssODNs that were end-protected by phosphorothioate (PTO) linkages caused increased H2AX phosphorylation and impaired cell cycle progression in both corrected and non-corrected cells due to induction of genomic DSBs. Our results demonstrate that the use of unmodified rather than PTO end-protected ssODNs allows stable gene modification without compromising the genomic integrity of the cell, which is crucial for application of ssODN-mediated gene targeting in (embryonic) stem cells.

INTRODUCTION

Gene targeting by single-stranded oligodeoxyribonucleotides (ssODNs) is a promising tool for introducing site-specific sequence alterations into the genome of

mammalian cells. The procedure only requires short synthetic ssODNs that are homologous to the target locus, except for a single or a few centrally located bases that comprise the desired genetic alteration. Although the exact mechanism underlying ssODN-mediated gene targeting remains elusive, several reports have demonstrated the involvement of DNA replication. Synchronizing cells in the S phase of the cell cycle or reducing the rate of replication fork progression improved the targeting frequency in various cell types (1–4). It has therefore been postulated that the ssODN anneals to its complementary genomic target sequence within the context of a replication fork. Extension of the ssODN by the replication machinery would result in incorporation of the ssODN into the newly synthesized DNA strand (5,6). Following annealing, DNA mismatches are formed between the ssODN and its chromosomal complement. We have previously shown that these mismatches are recognized and removed by the DNA mismatch repair (MMR) system, thereby preventing introduction of the desired genetic alteration. Deletion or down-regulation of the central MMR gene *Msh2* dramatically improved the targeting frequency in mouse embryonic stem cells (ESCs) (7,8). Recently, this inhibitory effect of the MMR system has been confirmed in human hepatocytes (9), CHO-K1 cells (10) and HEK293T L α cells (11). The involvement of the MMR system, which functions to correct replication errors that escape proofreading, provides an additional indication for ssODN-mediated gene targeting to take place during replication.

Many reports have demonstrated the feasibility of ssODN-mediated gene targeting using mutant *EGFP* reporter systems in a variety of cell lines (2,10–14). From experiments using *EGFP* reporters some general conclusions have been drawn: (i) anti-sense ssODNs complementary to the non-transcribed strand were most effective (1,3,12,13); (ii) protection of ssODNs against nucleolytic degradation by phosphorothioate (PTO) linkages (10,12) or locked nucleic acid (LNA) bases (15) enhanced the targeting frequency; (iii) correction by

*To whom correspondence should be addressed. Tel: +31 20 512 20 84; Fax: +31 20 669 13 83; Email: h.t.riele@nki.nl

PTO-modified ssODNs triggered a DNA damage response, including activation of the ATM/ATR pathway and phosphorylation of histone H2AX, due to the formation of genomic double-stranded DNA breaks (DSBs) (11,13,14). As a result, most of the corrected cells arrested in the S (14) or G₂ phase (2,10,11) of the cell cycle and were rapidly diluted by the proliferating uncorrected cells in the population. Remarkably, these conclusions did not match the results we have obtained previously using a mutant *neo* reporter ESC line, in which the formation of G418-resistant colonies served as readout for the targeting frequency: in our *neo* ESC line, sense ssODNs performed better than anti-sense ssODNs and PTO modifications decreased the targeting frequency (7,16). It is unclear whether these discrepancies are due to the use of different reporter systems and different cell types. In particular, it is important to assess whether ESCs modified by ssODN-mediated gene targeting suffer from DNA damage as such cells need to retain pluripotency and germ line competence to allow the generation of mutant mice (8,17).

In the present study, we have generated a novel *Msh2*-deficient mouse ESC line that carries a single copy of a mutant *EGFP* reporter gene at the same chromosomal position as the previously described mutant *neo* reporter gene (7,8,16). This *EGFP* reporter cell line enabled us to monitor gene correction events already 24 h after ssODN exposure and to study the fate of corrected cells upon further culturing. Specifically, we have compared the fate of cells corrected by either sense or anti-sense ssODNs. This experiment provided strong support for a model in which sequence alteration occurs through incorporation of the ssODN into the genome during DNA replication. Importantly, gene targeting by unmodified ssODNs only mildly affected the viability of the targeted cells, which may facilitate future therapeutic applications.

MATERIALS AND METHODS

Cell culture conditions

129/*Ola*-derived E14-IB10 ESCs were cultured on MEF feeders in Glasgow minimal essential medium supplemented with 10% foetal calf serum (FCS), 1 mM sodium pyruvate, 1× non-essential amino acids, 1 mM 2-mercaptoethanol and 1000 U per milliliter of leukemia inhibitory factor. For transfections and antibiotic selections, ESCs were cultured onto gelatin-coated plates in BRL (buffalo–rat liver cells)-conditioned medium.

Neo reporter cell line

We developed a selectable mutant neomycin (*neo*) reporter cell line in which the start codon of the *neo* resistance gene was mutated from ATG to AAG (Figure 1). A single copy of the mutant *neo* reporter gene was stably integrated into the *Rosa26* locus of *Msh2*-deficient ESCs as described earlier (7).

EGFP reporter cell lines

Plasmid pEGFP-N1 carries the enhanced green fluorescent protein (EGFP) ORF under the control of the

CMV IE promoter/enhancer (Clontech). The coding sequence of *EGFP* without start codon was amplified by PCR from pEGFP-N1 using primers 5'-CGAGGTTACCA TGTGAGCAAGGGCGAGGA-3' and 5'-CTAGAGTC GCGGCCGCTTTAC-3' to introduce KpnI and NotI sites (underlined). To generate a mutant *EGFP* start region, we annealed two synthetic DNA oligonucleotides encoding the start region of the mutant *neo* reporter in order to obtain a double-stranded DNA fragment with BglII and KpnI overhangs (5'-GATCTGACCCAATTC TAGAGCCGCCACCAAGGCCTATGCATCGAGCTT GGATGGATTGCACGCAGGGTAC-3'). The mutant *EGFP* start region was ligated together with the KpnI/NotI-digested *EGFP* PCR product (without start region) into the BglII and NotI sites of pEGFP-N1. Similarly, a plasmid with a wild-type (WT) start region (ATG instead of AAG) was constructed for control purposes. Subsequently, the 1.7-kb pCMV-*EGFP*-SV40pA fragment was amplified using the Expand Long Template PCR system (Roche) and primers 5'-CCGCTC GAGATTAATAGTAATCAATTACGGGGT-3' and 5'-CCGCTCGAGCTTAAGATACATTGATGAGTTTG G-3' and inserted into the XhoI site of the *Rosa26*-*His* targeting vector.

A single copy of the mutant and WT *EGFP* gene was stably integrated into the *Rosa26* locus of *Msh2*-deficient ESCs as described earlier (7). Single copy integration was confirmed by Southern blot analysis.

Transfection

ssODNs were transfected following the TransFast-mediated transfection method described earlier (8). Briefly, 7 × 10⁵ ESCs were seeded onto a gelatin-coated 6-well in BRL-conditioned medium the day before transfection. For one well, 3 μg of ssODNs and 27 μl of TransFast transfection agent (Promega) were diluted in 1.4 ml FCS-free medium and incubated for 15 min at room temperature. After 75 min of exposure to the transfection mixture at 37°C, 4 ml of BRL-conditioned medium with FCS was added to the cells. Cells were harvested for flow cytometry at the indicated time points after transfection. The targeting frequency is the number of EGFP-positive cells per 10⁵ cells that were analysed by flow cytometry.

Cells were exposed to 50 μM hydroxyurea (Sigma-Aldrich) for 6 h prior to ssODN transfection and for another 22 h during ssODN exposure.

Oligonucleotides

ssODNs were designed to correct the mutant start region of the *neo* or the *EGFP* reporter gene by introducing an in-frame ATG start codon (sequences of sense ssODNs are listed in Figure 1). Anti-sense ssODNs introduce identical base changes but have opposite polarity (i.e. are complementary to the non-transcribed strand). When indicated, ssODNs were modified with either three PTO linkages or a single LNA base on each end to protect them against nucleolytic degradation. ssODNs were purchased from Sigma-Aldrich and Eurogentec.

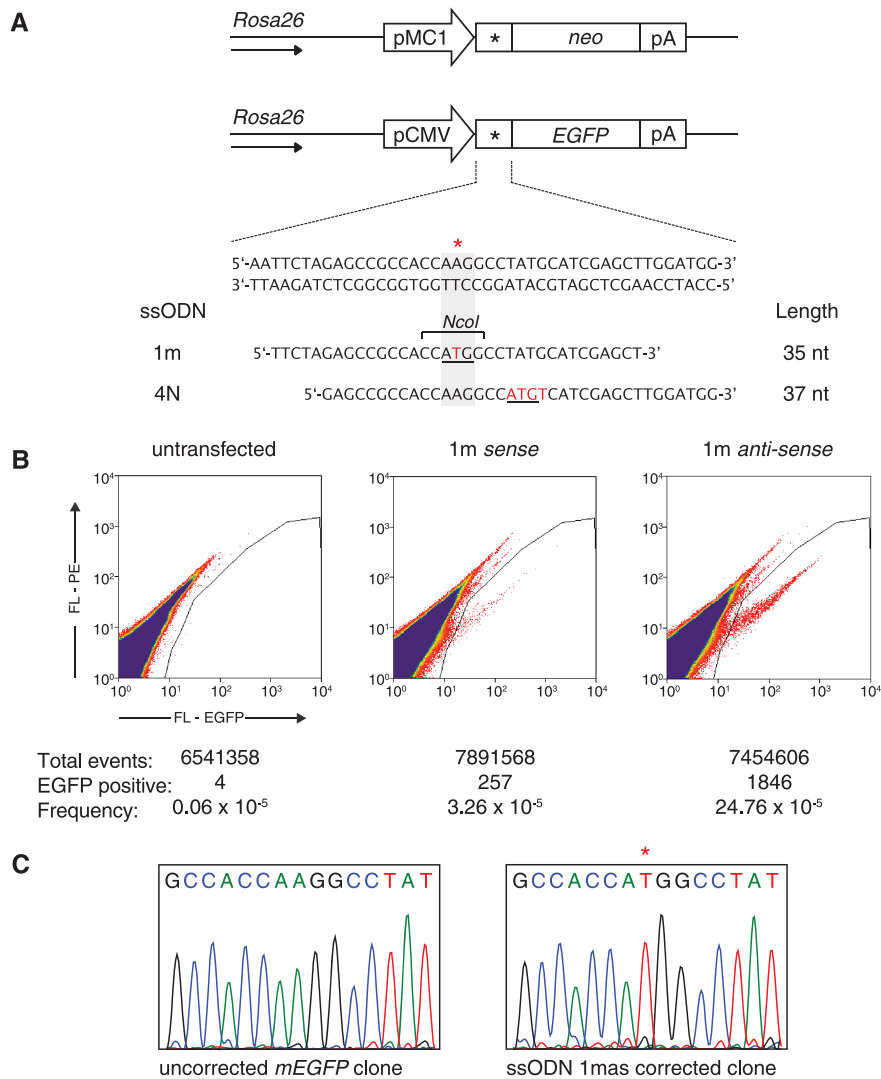


Figure 1. Correction of a mutant *EGFP* reporter gene by ssODNs. (A) Sequence of the mutant *neomycin* (*neo*) and *EGFP* reporter genes in which the start codon (ATG) is replaced for AAG (Asterisk). Activity of the reporter genes can be restored by ssODNs that substitute one (1m) or 4 nt (4N) (indicated in red) to create a new ATG start codon (underlined). Sequences of sense ssODNs complementary to the transcribed strand are shown. Arrow indicates the direction of the *Rosa26* promoter. *NcoI* indicates the restriction site that is generated by correction with ssODN 1m. (B) Representative flow cytometry dot plots of *Msh2*^{-/-} *mEGFP* cells either untransfected (left panel) or transfected with ssODN 1m sense (middle panel) or 1m anti-sense (right panel) analysed 24 h after ssODN transfection. (C) Sequence analysis of genomic DNA showing precise correction by ssODN 1m.

Restriction enzyme and sequence analysis of the *EGFP* region

Msh2^{-/-} *mEGFP* ESCs were exposed to unmodified anti-sense ssODN 1m for 24 h after which the EGFP-positive cells were separated by flow cytometry. After genomic DNA isolation, the *EGFP* region was amplified by PCR and the resulting products were cloned into pGEM-T Easy (Promega). DNA from 115 clones was digested with the diagnostic restriction enzyme *NcoI*. Sequence analysis of the *EGFP* region confirmed the presence of the ssODN-directed nucleotide alteration.

Flow cytometry

Quantification of EGFP-positive cells was performed on a CyAn ADP flow cytometer using Summit V4.3.01

software for analysis (DAKO Cytomation). Cells were harvested 24 h after transfection and resuspended in PBS supplemented with 0.1% FCS and DAPI (4',6'-diamidino-2-phenylindole) in order to exclude dead cells from the analysis. Cells were gated based on cell size (FSC/SSC), doublet discrimination (pulse width/SSC) and viability (DAPI/SSC). For each sample $\sim 4 \times 10^6$ cells were acquired and analysed.

Cell sorting

Cell sorting was conducted on a BD FACSAria flow cytometer (BD Biosciences). Cells were harvested 24 h after ssODN transfection and resuspended in PBS supplemented with 2% FCS. Cells were separated by a FSC/SSC amplitude gate; doublets were excluded by FSC/SSC width gates.

To determine the colony survival of corrected cells, *Msh2*^{-/-} *mEGFP* ESCs were exposed to various types of anti-sense ssODN 1m for 24 h and separated into 2000 EGFP-positive and -negative cells. For control purposes, *Msh2*^{-/-} WT *EGFP* ESCs were mixed with EGFP-negative *Msh2*^{-/-} *mEGFP* ESCs and subsequently sorted. The sorted cells were plated onto three gelatin-coated 100 mm dishes. After 8–10 days, surviving colonies were stained with Leishman's eosin methylene blue solution (Merck) and counted. The colony survival of EGFP-positive cells was normalized to the colony survival of EGFP-negative cells that had been exposed to the same ssODNs.

For the Cy5-ssODN uptake experiments, *Msh2*^{-/-} *neo* ESCs were transfected with 5'-Cy5-labelled sense ssODN 4N mixed with unlabelled sense ssODN 4N (ratio 1:4). The day after transfection, cells were binned into four separate groups based on their Cy5 fluorescence signal [mean Cy5 fluorescence (a.u.) in *bin 1*, 1×10^3 ; *bin 2*, 4.6×10^3 ; *bin 3*, 1.2×10^4 ; *bin 4*, 3.5×10^4]. Approximately 2.0 – 2.5×10^6 cells were sorted per bin in two replicate runs per experiment. For each bin, cells were plated onto two gelatin-coated 100 mm dishes at 1000 cells/dish to assess their colony-forming ability. The remainder of the cells was plated for G418 selection onto three gelatin-coated 100 mm dishes to determine the targeting frequency. G418 selection (800 μ g/ml; GIBCO-Invitrogen) was started 24 h after sorting. After 8–10 days, surviving colonies were stained and counted. Targeting frequencies were calculated by dividing the number of G418-resistant colonies by the number of cells that were plated after sorting.

MPM2 staining

After exposure to anti-sense ssODN 1m for 24 h, *Msh2*^{-/-} *mEGFP* ESCs were treated with nocodazole (250 ng/ml) for 12 h and harvested. Cells were fixed in 1% paraformaldehyde for 15 min on ice, washed and permeabilized in 90% ice-cold methanol and stored at -20°C for at least 2 h. Cells were washed three times with 1% BSA in PBS and incubated with anti-MPM2 antibody (1:100; Upstate Biotechnology) in 5% BSA, 0.2% Triton X-100 in PBS overnight at 4°C . After two washing steps in 1% BSA/PBS, cells were subsequently stained with Cy5-conjugated anti-mouse antibody and counterstained with DAPI. EGFP and Cy5 fluorescence were simultaneously quantified on a CyAn ADP flow cytometer. For each sample, 1 – 3×10^6 cells were acquired.

Analysis of H2AX phosphorylation

Msh2^{-/-} *mEGFP* ESCs were exposed to anti-sense ssODN 1m for 24 h and fixed and permeabilized as described earlier. Cells were incubated with Alexa Fluor 647-conjugated γ -H2AX (Ser 139) antibody (1:50; Cell Signaling Technology Inc.) in 5% BSA, 0.2% Triton X-100 in PBS overnight at 4°C . After two washing steps in 1% BSA/PBS, cells were counterstained with DAPI. EGFP and Alexa Fluor 647 fluorescence were simultaneously quantified on a CyAn ADP flow cytometer.

Mock-transfected *Msh2*^{-/-} *mEGFP* cells (without ssODN), *Msh2*^{-/-} WT *EGFP* cells and *Msh2*^{-/-} *mEGFP* cells exposed to 10 μ M etoposide for 4 h were included as controls. For each sample, at least 2×10^4 of the control cells and 1 – 2×10^6 of the ssODN-transfected cells were acquired.

Neutral comet assay

Msh2^{-/-} *mEGFP* ESCs were exposed to unmodified or PTO-modified anti-sense ssODN 1m for 24 h and separated into EGFP-positive and EGFP-negative cells by flow cytometry. Mock-transfected *Msh2*^{-/-} *mEGFP* cells (without ssODN), *Msh2*^{-/-} WT *EGFP* cells, and *Msh2*^{-/-} *mEGFP* cells exposed to 25 Gy of γ -irradiation were included as controls. The neutral comet assay was performed as previously described (18). Briefly, ~ 8000 sorted cells from each population were resuspended in 1.2 ml 0.75% low-gelling-temperature agarose (Sigma-Aldrich) at 40°C and pipetted onto glass slides pre-coated with agarose. After gelling for 2 min, slides were immersed into N1 lysis buffer (2% sarkosyl, 0.5 M Na₂EDTA, 0.5 mg/ml proteinase K) and incubated at 37°C in the dark for 22 h. After lysis, slides were rinsed three times in N2 solution (90 mM Tris, 90 mM boric acid, 2 mM Na₂EDTA pH8.5) for 30 min at RT. Then, electrophoresis was conducted in fresh N2 solution for 25 min at 0.6 V/cm. Slides were stained in 2.5 μ g/ml propidium iodide for 20 min. Images were captured using a Zeiss AxioObserver Z1 inverted fluorescence microscope equipped with a Hamamatsu ORCA-ER B/W CCD camera using identical exposure settings. Images were processed using AxioVision software (Zeiss). The comets tail moment (TM) was determined using the CASP software, version 1.2.2 (www.casp.of.pl). For each sample, the TM of at least 80 randomly chosen cells was measured.

RESULTS

Reporter cell lines

To monitor the frequency of ssODN-mediated gene targeting, we used our previously described neomycin (*neo*) reporter system in which the *neo* gene was mutated by a single base substitution in the start codon (ATG to AAG; Figure 1A). In addition, we constructed a mutant *EGFP* (*mEGFP*) reporter gene of which the translational start site was replaced by the mutant *neo* start sequence (Figure 1A). Single copies of the mutant *neo* and the *mEGFP* genes were stably integrated into the *Rosa26* locus of *Msh2*-deficient mouse ESCs (7). ssODNs of 35–37 nt containing one (1m) or four (4N) centrally-located nucleotide substitutions were used to correct the mutant start sequence or to generate a novel ATG start codon, respectively. Gene correction by ssODN 1m also generates a diagnostic NcoI restriction site (Figure 1A). Correction of the *neo* reporter gene was monitored by the appearance of G418-resistant colonies after 8–10 days, while correction of the *mEGFP* reporter resulting in EGFP fluorescence could already be detected 24 h after ssODN transfection using flow cytometry (Figure 1B). NcoI restriction analysis of amplified genomic DNA

from sorted EGFP-positive cells after correction by anti-sense ssODN 1m confirmed that *EGFP* sequence correction had taken place at the chromosomal level (not shown). The accuracy of the sequence alteration was confirmed by sequence analysis (Figure 1C). These reporter systems allowed us to compare the frequency of ssODN-mediated gene targeting in mouse ESCs immediately and several days after exposure to ssODNs, providing information about the stability of the introduced sequence alteration, possible toxicity of the ssODNs and the viability of corrected cells.

Recovery of gene correction events varies with the time of readout

We used the *mEGFP* reporter gene to accurately compare the targeting efficacy of unmodified and chemically-modified ssODN 1m (Figure 2A) and ssODN 4N (Figure 2B). ssODNs were either in the sense or the anti-sense orientation with respect to transcription of the *mEGFP* gene. As previously shown for other mutant *EGFP* reporter cell lines (1,3,12,13), we found that anti-sense ssODNs appeared to be 5- to 20-fold more effective than sense ssODNs, when the number of EGFP-positive cells was determined 24 h after ssODN exposure (Figure 2A and B, black bars). Addition of three flanking PTO linkages or a single LNA base at each end to protect the ssODN against nucleolytic degradation improved the frequency, in particular of anti-sense ssODNs. Remarkably however, when EGFP expression was analysed 8 days after ssODN exposure, the targeting frequency of anti-sense ssODNs had dramatically decreased, whereas the targeting frequency of sense ssODNs had increased (Figure 2A and B, grey bars). The strand bias was now in favour of the sense ssODNs, which is in agreement with our previous results using the *neo* reporter system (16). Particularly, PTO-modified anti-sense ssODNs, although being the most effective at 24 h after ssODN exposure, showed the strongest reduction in the number of EGFP-positive cells after 8 days (39- versus 6-fold reduction for unmodified anti-sense ssODN 1m, Figure 2A).

Physical incorporation of ssODNs during DNA replication

Different models have been proposed for the mechanism of ssODN-mediated gene targeting [reviewed in ref. (19)]. In one model (Figure 8A, model I), the ssODN anneals to its chromosomal complement and serves as a template for repair of this chromosomal DNA strand. If this were the case, anti-sense ssODNs would stimulate substitution of nucleotides at the non-transcribed strand, whereas sense ssODNs would lead to alteration of the transcribed strand. Support for such a model was obtained in murine myoblasts (20). In an alternative model (Figure 8A, model II), the ssODN becomes physically integrated into the genome within the context of either a D-loop or a replication fork. In this case, the reverse would take place: anti-sense ssODNs would lead to sequence alteration of the transcribed strand and sense ssODNs to alteration of the non-transcribed strand. Correction of the transcribed strand will lead to

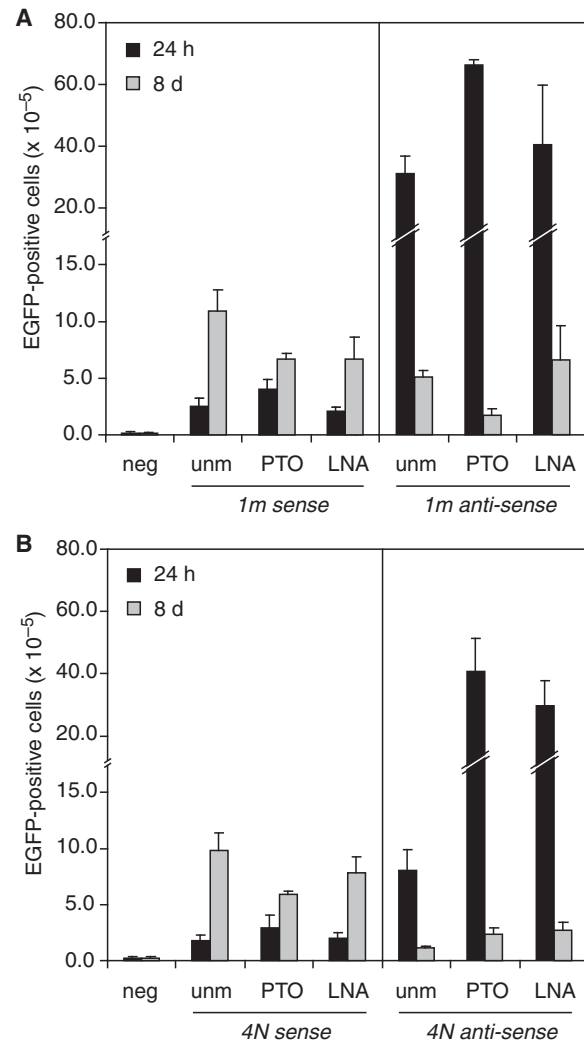


Figure 2. Gene correction frequencies by different types of ssODNs in *Msh2*-deficient *mEGFP* ESCs. (A) Unmodified (unm), PTO- and LNA-modified sense and anti-sense ssODN 1m were used to correct the *mEGFP* gene in *Msh2*-deficient ESCs. The number of EGFP-positive cells was determined 24 h (black bars) and 8 days (grey bars) after ssODN transfection. (B) Correction of the *mEGFP* gene by unmodified (unm), PTO- and LNA-modified sense and anti-sense ssODN 4N. Error bars represent the standard deviation (SD) of three independent experiments.

immediate EGFP expression, whereas correction of the non-transcribed strand will require an extra round of DNA replication to copy the base alteration(s) to the transcribed strand before EGFP expression can be detected.

To discriminate between these two models, we quantified the number of EGFP-positive cells either obtained with sense or with anti-sense ssODNs every 24 h over a period of 8 days. As shown in Figure 3A (black bars), the targeting frequency of sense ssODN 1m was only $3.0 \pm 1.6 \times 10^{-5}$ at the 24 h time point (Day 1), but sharply increased to a maximum of $14.5 \pm 1.9 \times 10^{-5}$ on Day 2. During the next two days, the number of EGFP-positive cells slightly decreased and stabilized at a frequency of $11.0 \pm 1.5 \times 10^{-5}$ on Day 4. Anti-sense

ssODN 1m showed the maximum targeting frequency ($35.0 \pm 6.2 \times 10^{-5}$) already on Day 1 (Figure 3B, black bars), after which the number of EGFP-positive cells gradually decreased until Day 4–5 and stabilized at a frequency of $4.5 \pm 0.4 \times 10^{-5}$. These observations indicate that the genetic modification induced by sense ssODNs required an extra round of DNA replication to become expressed, supporting the model that the sense ssODNs became physically integrated into the non-transcribed strand. The immediate EGFP-positivity observed with the anti-sense ssODNs indicates that these ssODNs had integrated into the transcribed strand.

This model provides a simple explanation for the decline of EGFP-positive cells obtained following exposure to anti-sense ssODNs (Figure 3B). Incorporation of anti-sense ssODNs into the transcribed strand immediately provides a template for EGFP production, probably already in the G₂ phase of the cell cycle (Figure 8C). However, in these cells only one of the four single DNA strands contains the corrected start codon. To confirm this, we amplified the genomic *EGFP* region from EGFP-positive cells that were sorted 24 h after exposure

to anti-sense ssODN 1m. Individual fragments were cloned and analysed for the presence of the diagnostic NcoI site, indicative of the ssODN-mediated sequence correction. Indeed, 24 out of 115 analysed clones (21%) contained the NcoI site, which is in fair agreement with modification of only one of the four DNA strands (Figure 8C, day 1). Subsequent semi-conservative DNA replication and cell division will gradually dilute the number of EGFP-positive cells, theoretically 4-fold. In contrast, cells corrected by sense ssODNs, need to replicate their DNA once to transmit the genetic modification to the transcribed strand (Figure 8B), which is reflected by the sharp increase in EGFP-positive cells on Day 2 (Figure 3A). The modest decline of EGFP-positive cells, which we reproducibly observed at Day 4, indeed indicates that EGFP was expressed in G₂ cells immediately after the corrected start codon was transmitted to the transcribed strand. Because EGFP has a half-life of ~24 h (21), the fluorescent signal may be transmitted to both daughter cells and slowly fade in one cell, while the other carries the corrected DNA template and will stably express EGFP fluorescence (Figure 8B and C).

These observations confirm our previous hypothesis that ssODN-mediated gene targeting in mouse ESCs occurs within the context of a replication fork. Incorporation of the sense ssODN into the lagging strand, which is more accessible during DNA replication than the leading strand, could explain the observed supremacy of sense over anti-sense after 8 days (Figure 3). We have previously shown that hydroxyurea treatment resulted in enhanced targeting frequencies in *Msh2*^{-/-} *neo* ESCs (16). Hydroxyurea causes depletion of intracellular dNTPs, which reduces the rate of DNA synthesis (22). Slowing down replication fork progression may increase the exposure of the single-stranded DNA regions that are present during replication, particularly in the lagging strand. Here, we investigated the effect of hydroxyurea on the frequency of sense and anti-sense ssODN-mediated correction of the *mEGFP* reporter over a time course of 8 days. *Msh2*^{-/-} *mEGFP* ESCs were incubated with 50 μM hydroxyurea between 6 h before and 22 h after ssODN exposure. For sense ssODN 1m, hydroxyurea treatment resulted in a 1.5-fold increase in targeting frequency (Figure 3A, grey bars), confirming our results obtained with the *neo* reporter (16). However, the targeting frequencies of anti-sense ssODN 1m were not significantly altered upon hydroxyurea treatment (Figure 3B, grey bars). The observation that hydroxyurea augmented the accessibility of the target locus to sense ssODNs, strongly suggests that these ssODNs were incorporated into the lagging strand.

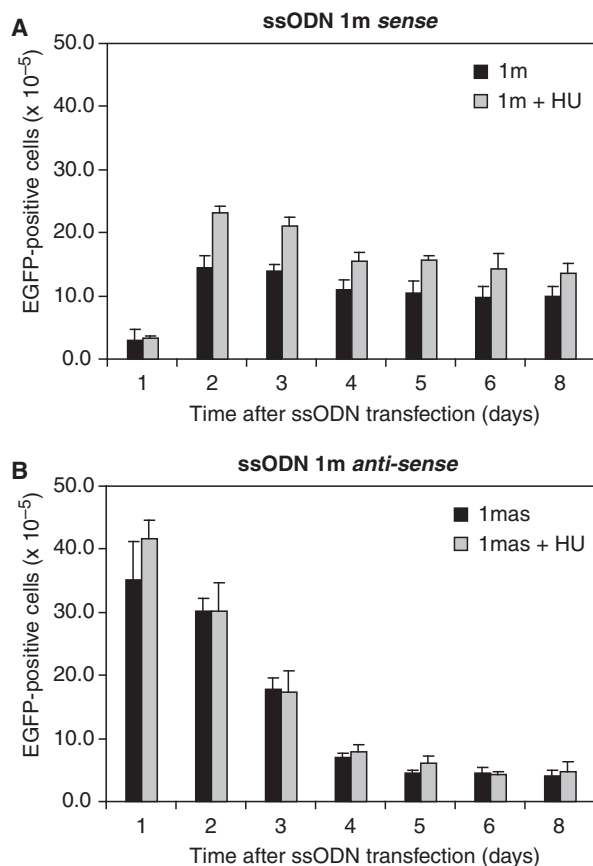


Figure 3. Time course of recovery of EGFP-positive cells obtained by unmodified ssODN 1m. *Msh2*^{-/-} *mEGFP* ESCs were exposed to ssODN 1m without treatment (black bars), or in the presence of 50 μM hydroxyurea (HU; grey bars). The number of EGFP-positive cells was quantified by flow cytometry at the indicated time points after transfection. Error bars represent the SD of four independent experiments. (A) Correction by unmodified sense ssODN 1m (1m). (B) Correction by unmodified anti-sense ssODN 1m (1mas).

Unmodified ssODNs only mildly reduced the survival of corrected cells

The gradual loss of EGFP-positive cells upon gene correction by anti-sense ssODNs as shown in Figure 3B, has also been observed by others (2,11,14). In these experiments, cells corrected by PTO-modified ssODNs showed a reduced viability due to high levels of DNA damage. We therefore investigated whether ssODN-mediated gene

targeting *per se* affected the viability of cells. Twenty-four hours after exposure of *Msh2*^{-/-} *mEGFP* ESCs to various types of anti-sense ssODN 1m, EGFP-positive and -negative cells were separated by flow cytometry and plated to determine their colony-forming ability. For all types of ssODNs, the viability of EGFP-positive cells was reduced compared to EGFP-negative cells (Figure 4). However, *Msh2*^{-/-} ESCs expressing a WT *EGFP* gene showed 75% survival compared to EGFP-negative *Msh2*^{-/-} *mEGFP* reporter cells, indicating that EGFP expression itself already reduced cell viability. Corrected for EGFP toxicity, we found that 73% of EGFP-positive cells obtained with unmodified or LNA-modified ssODNs were able to form colonies. In contrast, only 27% of the EGFP-positive cells obtained with PTO-modified ssODNs survived. Thus, the apparent loss of cells corrected by unmodified anti-sense ssODNs observed in Figure 3B can largely be explained by dilution of the corrected DNA strand due to semi-conservative DNA replication and to a minor extent by reduced viability of the targeted cells. In contrast, the loss of cells corrected by PTO-modified ssODNs is aggravated by a strong reduction in cell viability.

ssODN uptake did not affect survival

The reduced viability of corrected cells may be due to toxicity of high levels of ssODNs in cells. To investigate whether unmodified ssODNs conferred toxicity, we determined the cell viability as a function of the level of ssODN uptake. *Msh2*^{-/-} *neo* cells were exposed to 5'-Cy5-labelled sense ssODN 4N and sorted into four equal bins based on their Cy5 fluorescence signal 24h after transfection. After sorting, part of the cells was plated to assess their colony-forming ability, while the remainder of the cells was subjected to G418 selection to

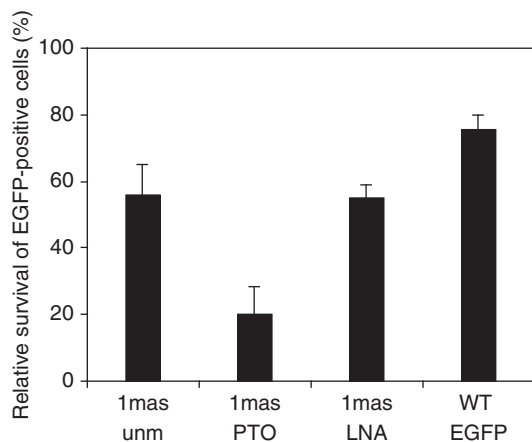


Figure 4. Relative colony survival of EGFP-positive cells. Colony-forming ability of EGFP-positive *Msh2*^{-/-} *mEGFP* ESCs after correction by unmodified (unm), PTO-modified and LNA-modified anti-sense ssODN 1m (1mas). *Msh2*^{-/-} ESCs carrying a wild-type (WT) *EGFP* gene were used as control. The colony survival of the corrected EGFP-positive cells was normalized to the colony survival of uncorrected EGFP-negative cells that had been exposed to the same ssODNs. Error bars represent the SD of two independent experiments.

determine the targeting frequency. Although the sorting procedure reduced the colony-forming ability of ESCs, there was no correlation between cell viability and the level of Cy5-ssODN uptake (Figure 5A). Thus, cells with a high Cy5-ssODN uptake (bin 4) were as viable as cells with a low uptake (bin 1), indicating that the presence of unmodified ssODNs in cells did not affect cell viability. On the other hand, increased Cy5-ssODN uptake did result in an increased targeting frequency, as reported previously (23). Cells with a 10- to 100-fold higher Cy5-ssODN uptake (bin 4 compared to bin 1) showed a 4-fold higher targeting frequency (Figure 5B).

Cells corrected by unmodified ssODNs progress into mitosis

Another explanation for the reduced viability of corrected cells could be the accumulation of cells in the G₂ phase of the cell cycle, as has been reported previously (2,10,11). Due to the low targeting frequencies in mouse ESCs, we could not directly determine the cell cycle profile of corrected cells. Instead, we determined how many cells were able to progress into mitosis after ssODN-mediated correction of the *EGFP* gene. If ssODN-mediated gene correction leads to activation of a G₂ arrest, relatively less EGFP-positive cells will be able to progress into mitosis.

To address this question, *Msh2*^{-/-} *mEGFP* ESCs were exposed to unmodified or PTO-modified anti-sense ssODN 1m for 24h after which nocodazole was added for another 12h to arrest the cells in mitosis. Subsequently, cells were stained with MPM2 antibody to quantify the mitotic cells in the EGFP-negative and EGFP-positive population by flow cytometric analysis (Figure 6). Upon exposure to unmodified ssODNs, 44.2% of the uncorrected EGFP-negative cells had progressed into mitosis, which was comparable to mock-transfected (without ssODN) control cells (48.1%, data not shown). In the EGFP-positive population the percentage of mitotic cells was ~2-fold lower (23.4%), indicating that cell cycle progression was impaired upon correction by unmodified ssODNs. However, after correction by PTO-modified ssODNs only 9.8% of the corrected EGFP-positive cells had progressed into mitosis, which may be indicative of a more pronounced G₂ cell cycle arrest. Remarkably, the EGFP-negative cells that had been exposed to PTO-modified ssODNs also showed a reduced number of mitotic cells (34.6%), suggesting that exposure to PTO-modified ssODNs already interfered with cell cycle progression.

H2AX phosphorylation after ssODN-mediated gene targeting

Phosphorylation of histone H2AX on Ser-139 (γ -H2AX) occurs at sites flanking DNA DSBs and can be used as an indicator for the level of DNA damage within a cell (24,25). To investigate whether the impaired cell cycle progression was due to the activation of a DNA damage response, we have quantified the formation of γ -H2AX following ssODN exposure (Figure 7A). *Msh2*^{-/-} *mEGFP* ESCs were exposed to unmodified or PTO-modified anti-sense ssODN 1m for 24h after which

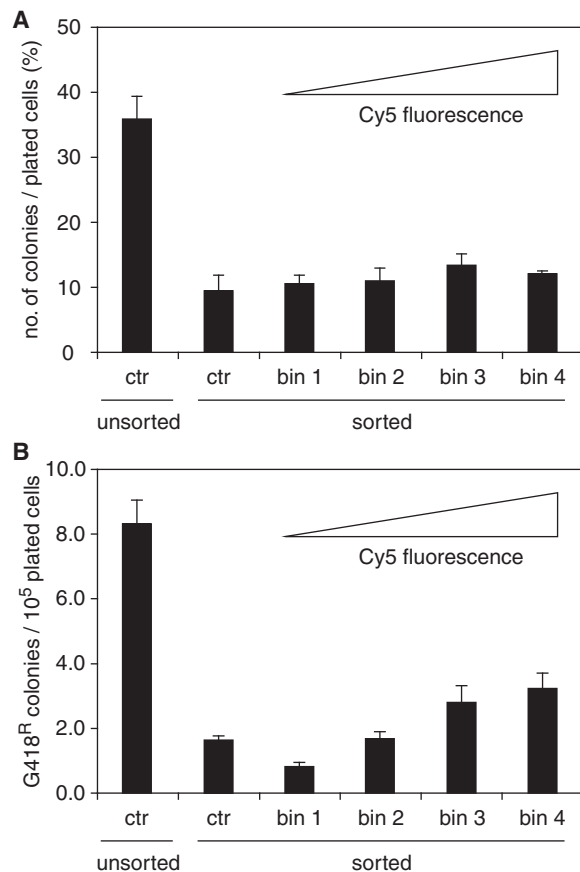


Figure 5. Effect of the level of ssODN uptake on colony survival and targeting frequency. *Msh2*^{-/-} *neo* ESCs were transfected with Cy5-labelled sense ssODN 4N and sorted into four equal bins based on their Cy5 fluorescence signal 24h after ssODN transfection (bin 1, 25% of cells with the lowest Cy5-ssODN uptake; bin 4, 25% of cells with the highest Cy5-ssODN uptake). *Msh2*^{-/-} *neo* ESCs transfected with Cy5-labelled sense ssODN 4N, either unsorted or sorted but not binned, were included as controls (ctr). (A) Colony survival of cells that were binned by their Cy5-ssODN uptake. (B) Targeting frequency of cells that were binned by their Cy5-ssODN uptake. Targeting frequency is the number of G418-resistant colonies per 10⁵ cells that were plated after sorting. Note that the calculated targeting frequencies after sorting are lower due to the reduced survival of the plated cells. Error bars represent the SD of two independent sorting experiments consisting of two replicate runs per sort.

γ -H2AX immunofluorescence and EGFP fluorescence were simultaneously measured by flow cytometry. As a control, etoposide-treated *Msh2*^{-/-} *mEGFP* cells displaying a high level of γ -H2AX (64.6%) were included in the analysis. As shown in Figure 7A, mock-transfected control cells already displayed an increased level of H2AX phosphorylation (8.7%), which may be due to the transfection procedure. In contrast, non-transfected *Msh2*^{-/-} WT *EGFP* cells displayed low γ -H2AX levels (0.2%), suggesting that EGFP expression itself did not activate a DNA damage response. Exposure to unmodified ssODNs did not lead to significant changes in H2AX phosphorylation in both the corrected EGFP-positive cells (5.9%) and the uncorrected EGFP-negative cells (6.3%) when compared to the mock-transfected control cells. However, following exposure to PTO-modified ssODNs,

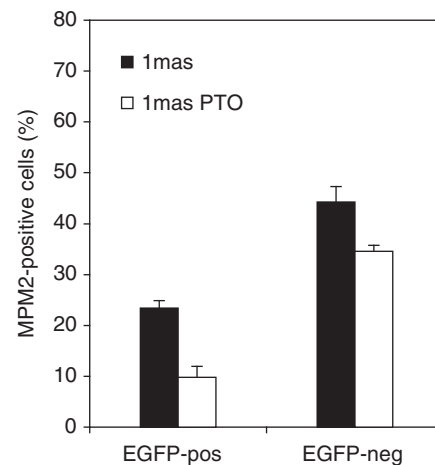


Figure 6. Mitotic entry following correction by ssODNs. *Msh2*^{-/-} *mEGFP* ESCs were transfected with unmodified or PTO-modified anti-sense ssODN 1m (1mas). After 24h, cells were treated with nocodazole for 12h, fixed and stained with anti-MPM2 antibody. MPM2-positive (mitotic) cells were quantified by flow cytometry in the EGFP-positive (pos) and EGFP-negative (neg) populations. Error bars represent SD of two independent experiments.

γ -H2AX levels in the EGFP-negative and -positive cells were 11.7 and 25.3%, respectively, indicating that exposure to and incorporation of PTO-modified ssODNs triggered a DNA damage response.

Unmodified ssODNs did not induce DNA damage in ESCs

It has been reported that correction by PTO-modified ssODNs resulted in an increased level of genomic DSBs (11,13,14). We have performed the neutral comet assay to determine whether exposure to or incorporation of unmodified ssODNs induced DSB formation. *Msh2*^{-/-} *mEGFP* ESCs were exposed to unmodified or PTO-modified anti-sense ssODN 1m for 24h. Subsequently, the EGFP-positive and -negative cells were separated by flow cytometry and subjected to the neutral comet assay (18). The amount of DNA damage was quantified by the TM, which represents the product of the tail length and the percentage of DNA in the comet tail (Figure 7B). After exposure to unmodified anti-sense ssODN 1m, there was no significant difference in the median TM value of the corrected EGFP-positive cells and the uncorrected EGFP-negative cells (8.4 versus 11.4, respectively) (Figure 7C). Moreover, mock-transfected *Msh2*^{-/-} *mEGFP* cells and *Msh2*^{-/-} WT *EGFP* control cells showed comparable TM values (9.4 and 10.6, respectively), indicating that exposure to or incorporation of unmodified anti-sense ssODN 1m had not induced a substantial amount of DNA damage. In contrast, the EGFP-positive cells that were corrected by PTO-modified anti-sense ssODN 1m showed high levels of DSBs (median TM = 39.4). A similarly high level of DSBs was found in control *Msh2*^{-/-} *mEGFP* cells that had been exposed to 25 Gy of γ -irradiation (median TM = 39.2). After exposure to PTO-modified ssODNs, even the uncorrected EGFP-negative cells showed

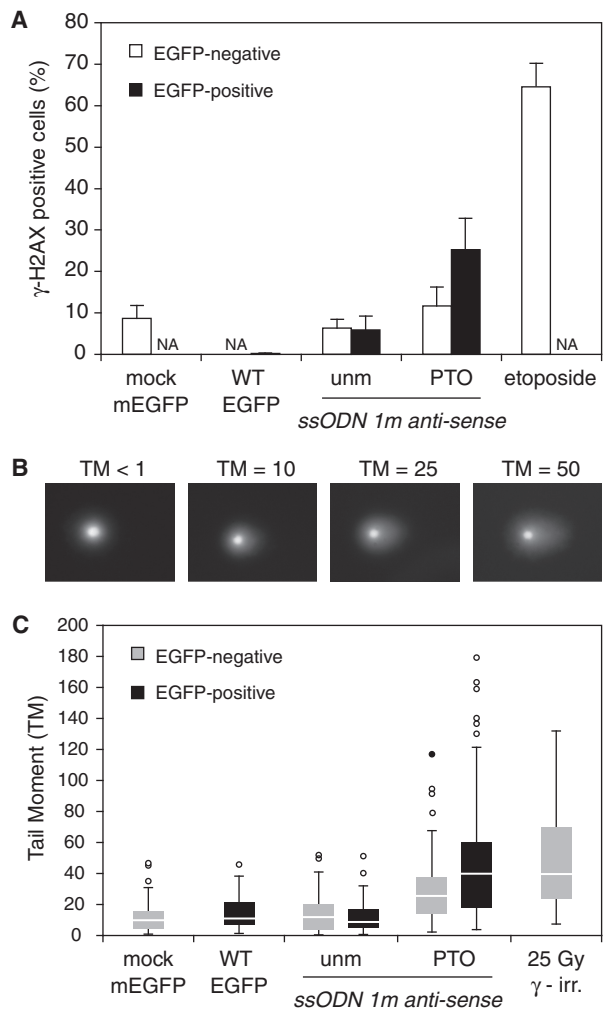


Figure 7. Quantification of DNA damage after ssODN-mediated gene targeting. (A) Quantification of H2AX phosphorylation. *Msh2*^{-/-} *mEGFP* ESCs were transfected with unmodified (unm) and PTO-modified (PTO) anti-sense ssODN 1m. After 24h, cells were fixed and stained with anti- γ -H2AX antibody. H2AX phosphorylation was quantified by flow cytometry in the corrected EGFP-positive and uncorrected EGFP-negative cells. Mock-transfected *Msh2*^{-/-} *mEGFP* cells (without ssODN), *Msh2*^{-/-} WT *EGFP* cells, and etoposide-treated *Msh2*^{-/-} *mEGFP* cells were included as controls. Error bars represent the SD of three independent experiments. (B) Representative images from the neutral comet assay performed on ssODN-transfected *Msh2*^{-/-} *mEGFP* ESCs with various levels of DNA damage as quantified by the tail moment (TM; % DNA in tail \times tail length). (C) Box plot representing the distribution of the comet tail moments after exposure to unmodified (unm) and PTO-modified anti-sense ssODN 1m. Corrected EGFP-positive and uncorrected EGFP-negative cells were separated by flow cytometry 24h after ssODN exposure and the level of DNA damage was quantified using the neutral comet assay. Mock-transfected *Msh2*^{-/-} *mEGFP* cells (without ssODN), *Msh2*^{-/-} WT *EGFP* cells and *Msh2*^{-/-} *mEGFP* cells exposed to 25 Gy of γ -irradiation were included as controls.

elevated TM values (median TM = 25.0), suggesting that both exposure to and incorporation of PTO-modified ssODNs led to DNA damage, which is in agreement with the γ -H2AX data (Figure 7A).

In summary, we have shown that correction by unmodified ssODNs did not induce a substantial amount of DNA damage and only marginally reduced the viability of

mouse ESCs, in sharp contrast to correction by PTO-modified ssODNs. Our results are most compatible with physical incorporation of the ssODN into the genome, most likely during DNA replication. Therefore, the decline of EGFP-positive cells corrected by unmodified anti-sense ssODNs was largely the consequence of semi-conservative replication rather than deleterious effects of ssODN exposure or incorporation.

DISCUSSION

In the present study, we have generated a novel *Msh2*-deficient mouse ESC line that carries a single copy integration of a mutant *EGFP* reporter gene at exactly the same position in the *Rosa26* locus as the mutant *neo* reporter gene we previously described (16). This *EGFP* reporter cell line enabled us to monitor gene correction events shortly after exposure of cells to ssODNs and importantly, to compare the fate of cells corrected by either sense or anti-sense ssODNs. We demonstrate that (i) ssODNs physically incorporated into the genome during DNA replication; (ii) PTO-modified ssODNs were deleterious to cells, while unmodified ssODNs only mildly affected cell viability; and (iii) unmodified ssODNs did not induce DNA damage.

Superiority of anti-sense ssODNs over sense ssODNs is a consequence of early readout

Using the *neo* reporter cell line, we have shown that the targeting frequency of sense ssODN 1m was $7.0 \pm 2.8 \times 10^{-5}$, while the targeting frequency of anti-sense ssODN 1m was $3.7 \pm 3.0 \times 10^{-5}$ (16). Here, using the novel *mEGFP* reporter ESC line, similar targeting frequencies were obtained when the number of EGFP-positive cells was determined 8 days after ssODN exposure (Figures 2A and 3), indicating that both reporter systems provided an accurate readout of the targeting frequency. Strikingly, by comparing the fate of cells corrected by either sense or anti-sense ssODNs, we noticed that the recovery of gene correction events was strongly influenced by the time of readout: initially anti-sense ssODNs performed best, while later sense ssODNs were most effective. We postulate that the initial strand bias indicates that ssODNs become incorporated into the genome: by incorporating into the transcribed strand and replacing the original genetic information, anti-sense ssODNs allow immediate detection of the corrected *EGFP* gene. In contrast, incorporation of the sense ssODNs into the non-transcribed strand requires the genetic alteration to be transferred to the transcribed strand before *EGFP* can be expressed (Figure 8B). Since the delay in EGFP expression was \sim 1 day (Figure 3A), it is most likely that this process occurred during DNA replication (Figure 8A, model II). As we have hypothesized before (16), the ultimate superiority of sense ssODNs over anti-sense ssODNs may be the result of the differential accessibility of the leading and lagging strand during replication. In our reporter system, it seems likely that sense ssODNs incorporated into the lagging strand.

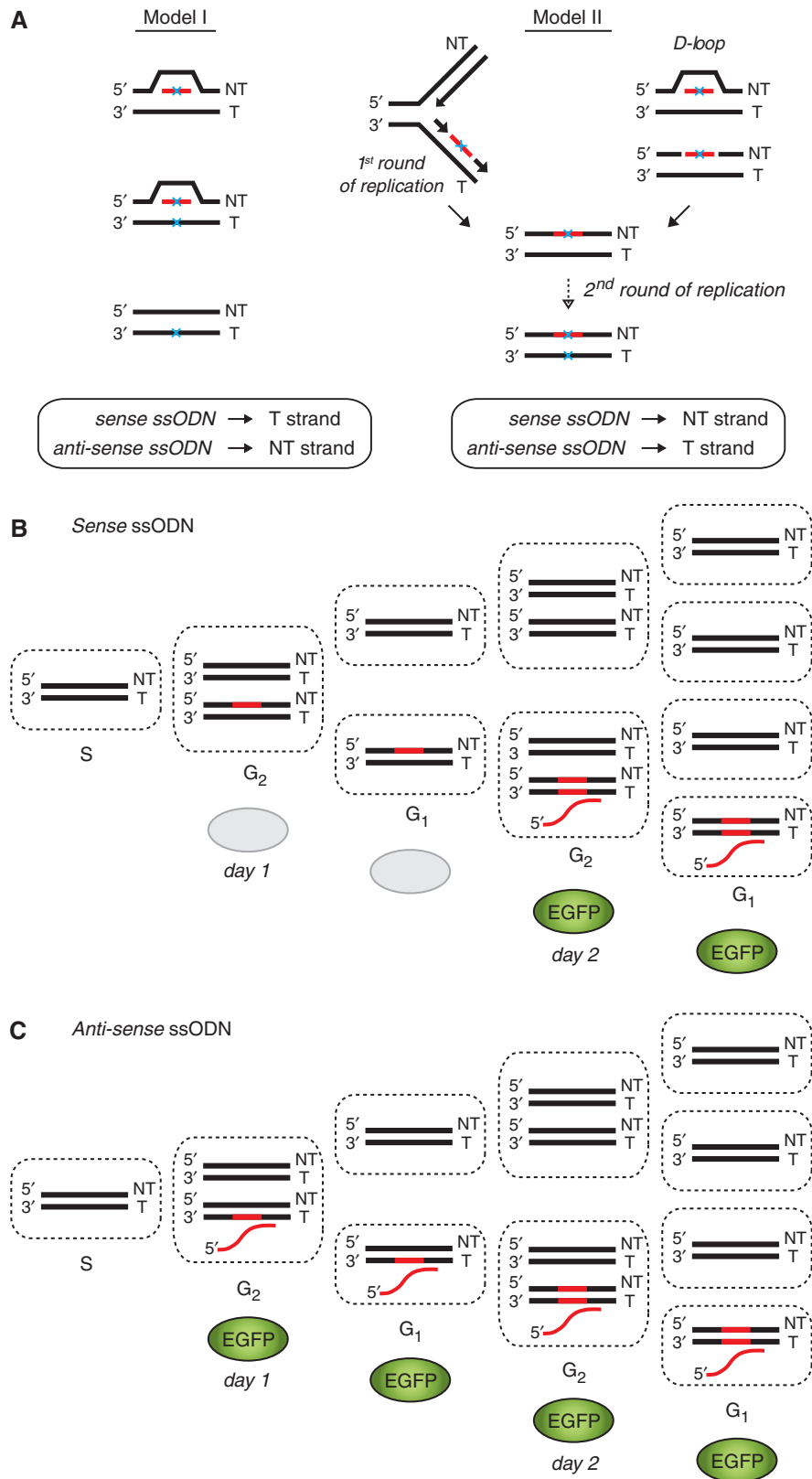


Figure 8. Model for ssODN-mediated correction of the *mEGFP* gene. (A) Hypothetical models for gene correction by sense ssODNs (indicated in red) in mouse ESCs. Model I: the ssODN anneals to its chromosomal complement and serves as a template for repair of this chromosomal DNA strand. If so, sense ssODNs would stimulate substitution of nucleotides (indicated by blue X) of the transcribed strand allowing immediate expression of EGFP. Model II: the ssODN becomes integrated into the genome within the context of either a replication fork or a D-loop. In this model, sense ssODNs would lead to sequence alteration of the non-transcribed strand. A second round of DNA replication is required to transfer the genetic alteration to the opposite strand to allow EGFP expression. Our findings are most compatible with integration of the ssODN during DNA

While our data are indicative of physical incorporation of the ssODN in ESCs during replication, in other cell types ssODN-mediated gene targeting may occur via replication-independent mechanisms. Using murine myoblasts, Bertoni *et al.* (20) demonstrated that after correction by methyl-CpG-modified *anti-sense* ssODNs, the appearance of EGFP-positive cells was delayed for 1 day. This suggests that in their system anti-sense ssODNs corrected the non-transcribed strand by a repair-dependent mechanism as shown in Figure 8A, model I.

Unmodified ssODNs only mildly reduced the viability of corrected cells and did not induce DNA damage

The addition of PTO linkages enhanced the targeting frequency of particularly anti-sense ssODNs at 24 h after transfection (Figure 2), probably by protecting the ssODNs against nucleolytic degradation. However, after 8 days, PTO-modified anti-sense ssODNs showed the most dramatic decrease in targeting frequency. We have demonstrated that cells corrected by PTO-modified ssODNs displayed a strongly reduced colony-forming ability, an impaired cell cycle progression and activation of a DNA damage response, which appeared to be consequences of an increased level of unrepaired genomic DSBs, as has been reported previously (11,13). Strikingly, our results imply that the observed DNA damage response was specific for gene correction by PTO-modified ssODNs and did not occur when unmodified ssODNs were used. First, the survival of cells corrected by unmodified ssODNs was only mildly affected when compared to cells expressing a WT *EGFP* gene (Figure 4). Second, the level of uptake of unmodified ssODNs did not affect the cell viability (Figure 5A). Third, EGFP-positive cells corrected by unmodified ssODNs showed similar low levels of DSBs as uncorrected EGFP-negative cells, as determined by the γ -H2AX response and the neutral comet assay (Figure 7).

In conclusion, we have developed a unique set of reporter cell lines carrying a single copy of either a mutant *neo* or a mutant *EGFP* gene at the same chromosomal position to study the short- and long-term effects of ssODN-mediated gene targeting. Using these cell lines, we could demonstrate that the strand bias in favour of anti-sense ssODNs was a consequence of early readout. Thus, reporter systems based on EGFP expression allow rapid recovery of gene correction events, but may be prone to misinterpretation. We provide strong evidence that ssODNs are incorporated during DNA replication. Importantly, we have shown that unmodified ssODNs do not induce a substantial amount of genomic DSBs. Our data imply that the apparent loss of targeted cells obtained by anti-sense ssODNs was merely the

consequence of semi-conservative replication and is therefore inherent to the targeting procedure. The use of unmodified ssODNs for gene targeting ensures stable outgrowth of targeted cells while preserving genomic integrity, features that are vital for application of this technique in (embryonic) stem cells.

ACKNOWLEDGEMENTS

We are grateful to Frank van Diepen and Anita Pfauth from the flow cytometry facility for their excellent technical support, and to Laurant Oomen and Lenny Brocks for help with fluorescence microscopy. We thank Sietske Bakker, Henri van de Vrugt and Eva Wielders for critical reading of the manuscript.

FUNDING

Grant from the Netherlands Genomics Initiative (Horizon Project 93516051). Funding for open access charge: The Netherlands Cancer Institute, Amsterdam, The Netherlands.

Conflict of interest statement. None declared.

REFERENCES

1. Brachman, E.E. and Kmiec, E.B. (2005) Gene repair in mammalian cells is stimulated by the elongation of S phase and transient stalling of replication forks. *DNA Repair*, **4**, 445–457.
2. Olsen, P.A., Randol, M. and Krauss, S. (2005) Implications of cell cycle progression on functional sequence correction by short single-stranded DNA oligonucleotides. *Gene Ther.*, **12**, 546–551.
3. Wu, X.S., Xin, L., Yin, W.X., Shang, X.Y., Lu, L., Watt, R.M., Cheah, K.S., Huang, J.D., Liu, D.P. and Liang, C.C. (2005) Increased efficiency of oligonucleotide-mediated gene repair through slowing replication fork progression. *Proc. Natl Acad. Sci. USA*, **102**, 2508–2513.
4. Engstrom, J.U. and Kmiec, E.B. (2008) DNA replication, cell cycle progression and the targeted gene repair reaction. *Cell Cycle*, **7**, 1402–1414.
5. Huen, M.S., Li, X.T., Lu, L.Y., Watt, R.M., Liu, D.P. and Huang, J.D. (2006) The involvement of replication in single stranded oligonucleotide-mediated gene repair. *Nucleic Acids Res.*, **34**, 6183–6194.
6. Radecke, S., Radecke, F., Peter, I. and Schwarz, K. (2006) Physical incorporation of a single-stranded oligodeoxynucleotide during targeted repair of a human chromosomal locus. *J. Gene Med.*, **8**, 217–228.
7. Dekker, M., Brouwers, C. and te Riele, H. (2003) Targeted gene modification in mismatch-repair-deficient embryonic stem cells by single-stranded DNA oligonucleotides. *Nucleic Acids Res.*, **31**, e27.
8. Aarts, M., Dekker, M., de Vries, S., van der Wal, A. and te Riele, H. (2006) Generation of a mouse mutant by oligonucleotide-mediated gene modification in ES cells. *Nucleic Acids Res.*, **34**, e147.
9. Igoucheva, O., Alexeev, V., Anni, H. and Rubin, E. (2008) Oligonucleotide-mediated gene targeting in human hepatocytes: implications of mismatch repair. *Oligonucleotides*, **18**, 111–122.

Figure 8. Continued

replication (Model II). NT, non-transcribed strand; T, transcribed strand. (B) Incorporation of sense ssODNs (indicated in red) into the non-transcribed strand during S phase requires an extra round of replication to transmit the corrected *EGFP* sequence to the transcribed strand (Day 2). After cell division, both daughter cells appear EGFP-positive although only one contains the corrected *EGFP* sequence. (C) In contrast, incorporation of anti-sense ssODNs (indicated in red) into the transcribed strand immediately provides a template for EGFP production, probably already in the G₂ phase of the cell cycle (Day 1). In these cells only one of the four DNA strands contains the corrected *EGFP* start codon. Subsequent semi-conservative DNA replication and cell division will gradually dilute the number of EGFP-positive cells, theoretically 4-fold.

10. Papaioannou, I., Disterer, P. and Owen, J.S. (2009) Use of internally nuclease-protected single-strand DNA oligonucleotides and silencing of the mismatch repair protein, MSH2, enhances the replication of corrected cells following gene editing. *J. Gene Med.*, **11**, 267–274.
11. Olsen, P.A., Solhaug, A., Booth, J.A., Gelazauskaite, M. and Krauss, S. (2009) Cellular responses to targeted genomic sequence modification using single-stranded oligonucleotides and zinc-finger nucleases. *DNA Repair*, **8**, 298–308.
12. Olsen, P.A., Randol, M., Luna, L., Brown, T. and Krauss, S. (2005) Genomic sequence correction by single-stranded DNA oligonucleotides: role of DNA synthesis and chemical modifications of the oligonucleotide ends. *J. Gene Med.*, **7**, 1534–1544.
13. Bonner, M. and Kmiec, E.B. (2009) DNA breakage associated with targeted gene alteration directed by DNA oligonucleotides. *Mutat. Res.*, **669**, 85–94.
14. Ferrara, L. and Kmiec, E.B. (2006) Targeted gene repair activates Chk1 and Chk2 and stalls replication in corrected cells. *DNA Repair*, **5**, 422–431.
15. Andrieu-Soler, C., Casas, M., Faussat, A.M., Gandolphe, C., Doat, M., Tempe, D., Giovannangeli, C., Behar-Cohen, F. and Concordet, J.P. (2005) Stable transmission of targeted gene modification using single-stranded oligonucleotides with flanking LNAs. *Nucleic Acids Res.*, **33**, 3733–3742.
16. Aarts, M. and te Riele, H. (2009) Parameters of oligonucleotide-mediated gene modification in mouse ES cells. *J. Cell Mol. Med.*, [Epub ahead of print, 20 July 2009].
17. Dekker, M., Brouwers, C., Aarts, M., van der Torre, J., de Vries, S., van de Vrugt, H. and te Riele, H. (2006) Effective oligonucleotide-mediated gene disruption in ES cells lacking the mismatch repair protein MSH3. *Gene Ther.*, **13**, 686–694.
18. Olive, P.L. and Banath, J.P. (2006) The comet assay: a method to measure DNA damage in individual cells. *Nat. Protoc.*, **1**, 23–29.
19. Engstrom, J.U., Suzuki, T. and Kmiec, E.B. (2009) Regulation of targeted gene repair by intrinsic cellular processes. *Bioessays*, **31**, 159–168.
20. Bertoni, C., Rustagi, A. and Rando, T.A. (2009) Enhanced gene repair mediated by methyl-CpG-modified single-stranded oligonucleotides. *Nucleic Acids Res.*, **37**, 7468–7482.
21. Li, X., Zhao, X., Fang, Y., Jiang, X., Duong, T., Fan, C., Huang, C.C. and Kain, S.R. (1998) Generation of destabilized green fluorescent protein as a transcription reporter. *J. Biol. Chem.*, **273**, 34970–34975.
22. Rosenkranz, H.S. and Levy, J.A. (1965) Hydroxyurea: a specific inhibitor of deoxyribonucleic acid synthesis. *Biochim. Biophys. Acta*, **95**, 181–183.
23. Murphy, B.R., Moayedpardazi, H.S., Gewirtz, A.M., Diamond, S.L. and Pierce, E.A. (2007) Delivery and mechanistic considerations for the production of knock-in mice by single-stranded oligonucleotide gene targeting. *Gene Ther.*, **14**, 304–315.
24. Rogakou, E.P., Pilch, D.R., Orr, A.H., Ivanova, V.S. and Bonner, W.M. (1998) DNA double-stranded breaks induce histone H2AX phosphorylation on serine 139. *J. Biol. Chem.*, **273**, 5858–5868.
25. Paull, T.T., Rogakou, E.P., Yamazaki, V., Kirchgessner, C.U., Gellert, M. and Bonner, W.M. (2000) A critical role for histone H2AX in recruitment of repair factors to nuclear foci after DNA damage. *Curr. Biol.*, **10**, 886–895.